FIBER LOOP MIRROR FILTER WITH TWO-STAGE HIGH BIREFRINGENCE FIBERS

K. S. Lim, C. H. Pua, and N. A. Awang

Department of Physics
Faculty of Sciences
University of Malaya
Malaysia

S. W. Harun

Department of Electrical Engineering
Faculty of Engineering
University of Malaya
Malaysia

H. Ahmad

Department of Physics
Faculty of Sciences
University of Malaya
Malaysia

Abstract—A fiber loop mirror (FLM) with two-stage high birefringence (Hi-Bi) fibers is theoretically and experimentally studied for various rotation angles and Hi-Bi fiber lengths. The experimental spectra are observed to be in good agreement with the theoretical spectra, verifying our theoretical model. The wavelength interval of the comb filter depends on the Hi-Bi fiber lengths and rotation angles. By varying the rotation angle from 0° to 90°, a comb-like transmission spectrum with small wavelength spacing is evolving into an exotic but periodic transmission spectrum and eventually become a larger wavelength spacing transmission spectrum. The FLM is useful in many applications such wavelength division multiplexing power equalization and management, switchable multi-wavelength fiber laser, optical switch and etc.

Corresponding author: S. W. Harun (swharun@um.edu.my).

1. INTRODUCTION

Fiber loop mirrors (FLMs) have been intensively developed and commonly used for many applications such as in all-optical signal processing and multi-wavelength fiber lasers [1–3]. This is attributed to their advantages such as low cost, low loss, simple construction and polarization independence [4, 5]. Tuning characteristic is one of the most important features especially when this filter is used in the fiber lasers and optical sensing. A FLM of one-stage high birefringence (Hi-Bi) fiber and polarization controller (PC) is a simple filter device, in which the filter spectrum depends on the PC and Hi-Bi fiber. However, the wavelength interval is only depends on the PMF [6]. The only way of varying the filter interval is to use different Hi-Bi fiber length in the FLM; it is not practical in real optical systems. To avoid the disadvantage, many techniques have been proposed theoretically and experimentally such as the use of multi sections of Hi-Bi fibers [7–9].

In this paper, a FLM of two-stage Hi-Bi fibers is proposed and the characteristics of this FLM are investigated both theoretical and experimentally. This FLM relies on two Hi-Bi fibers that are connected together at different angle of rotation in relation with the birefringence axes. A mathematical model of the loop mirror is constructed based on the Hi-Bi fiber segment lengths, rotation angle in the birefringence axes in the fiber and the effective refractive index difference of the Hi-Bi fiber. For verification of the mathematical model, the experimental results are obscured and compared with the analytical results. On the other hand, Fujikura FSM-45PM arc fusion splicer which is capable of fiber splicing at any precise angular alignment was used in the experiment to achieve accurate rotations of birefringence axes between Hi-Bi fiber segments.

2. EXPERIMENTAL SETUP AND THEORETICAL ANALYSIS

The proposed FLM with two-stage Hi-Bi fibers is schematically shown in Fig. 1. A polarisation insensitive 3 dB coupler is used to connect the ring cavity and the FLM. Two Hi-Bi fibers, namely HBF 1 and HBF 2, each length of L_1 and L_2 are used. The 'R' marks the splicing spot between the two fibers at a rotation angle of θ. The beam travels towards the first PC (PC1) and then 3 dB coupler at the input port, and the incident beam is split into two propagating beams. 50% of output beams travel clockwise around the loop; and the other 50% output beams travel counter-clockwise with a phase different of $\pi/2$. Two beams contrarily pass through PC2 and Hi-Bi fibers and
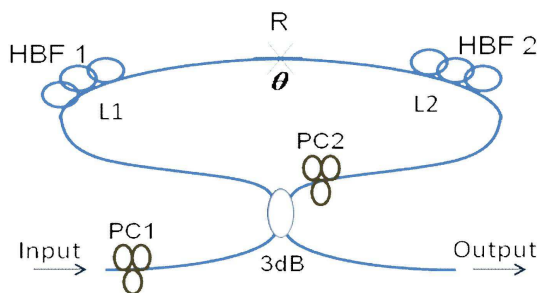
Figure 1. Schematic diagram of the FLM with two-stage Hi-Bi fibers.

the transmission spectrum is obtained at the output port as stated in Fig. 1.

To facilitate the theoretical analysis, the mathematical model for the FLM is constructed using Jones Matrix. The birefringence along the Hi-Bi fiber longitude fiber is assumed consistent except at the 'R' marked spliced spot where the rotation of birefringence axes occurs. In the first Hi-Bi fiber (HBF 1), the beam phases in the fast axes and slow axes can be written as

$$\phi_{1x} = \frac{2\pi n_x L_1}{\lambda} \tag{1}$$

and

$$\phi_{1y} = \frac{2\pi n_y L_1}{\lambda} \tag{2}$$

where n_x and n_y denote the refractive index in the fast axes and slow axes, λ is the beam wavelength. Similarly, the phases of the two orthogonal beam components in the second Hi-Bi fiber (HBF 2) can be expressed as

$$\phi_{2x} = \frac{2\pi n_x L_2}{\lambda} \tag{3}$$

and

$$\phi_{2y} = \frac{2\pi n_y L_2}{\lambda} \tag{4}$$

Let $E = \begin{pmatrix} E_x \\ E_y \end{pmatrix}$ denote the input beam of HBF 1 in the clockwise direction. After traveling through the HBF 1, the beam is phase retarded and the electric field is expressed as:

$$E_1 = \begin{pmatrix} e^{j\phi_{1x}} & 0 \\ 0 & e^{j\phi_{1y}} \end{pmatrix} \begin{pmatrix} E_x \\ E_y \end{pmatrix} \tag{5}$$

At location R, the polarization of the beam can be characterized as rotated by an angle of θ due to the rotation of birefringence axes in the HBF 2 with reference to previous fiber segment and the electric field can be represented as:

$$E_{1R} = \begin{pmatrix} \cos\theta & \sin\theta \\ -\sin\theta & \cos\theta \end{pmatrix} \begin{pmatrix} e^{j\phi_{1x}} & 0 \\ 0 & e^{j\phi_{1y}} \end{pmatrix} \begin{pmatrix} E_x \\ E_y \end{pmatrix} \qquad (6)$$

After traveling through HBF 2, the electric field of the beam eventually evolves into

$$E_{1R2} = \begin{pmatrix} e^{j\phi_{2x}} & 0 \\ 0 & e^{j\phi_{2y}} \end{pmatrix} \begin{pmatrix} \cos\theta & \sin\theta \\ -\sin\theta & \cos\theta \end{pmatrix} \begin{pmatrix} e^{j\phi_{1x}} & 0 \\ 0 & e^{j\phi_{1y}} \end{pmatrix} \begin{pmatrix} E_x \\ E_y \end{pmatrix} (7)$$

$$= \begin{pmatrix} E_x e^{j(\phi_{1x}+\phi_{2x})}\cos\theta + E_y e^{j(\phi_{1y}+\phi_{2x})}\sin\theta \\ -E_x e^{j(\phi_{1x}+\phi_{2y})}\sin\theta + E_y e^{j(\phi_{1y}+\phi_{2y})}\cos\theta \end{pmatrix} \qquad (8)$$

Assume that the input beam from the other arm of the coupler has the identical components magnitude. Analogously, the same result for the anti-clockwise propagating beam can be obtained by using the same algebraic manipulation.

$$E_{2R1} = \begin{pmatrix} E_x e^{j(\phi_{1x}+\phi_{2x})}\cos\theta + E_y e^{j(\phi_{1y}+\phi_{2x})}\sin\theta \\ -E_x e^{j(\phi_{1x}+\phi_{2y})}\sin\theta + E_y e^{j(\phi_{1y}+\phi_{2y})}\cos\theta \end{pmatrix} \qquad (9)$$

By adjusting PC2, the clockwise propagating beam E_{1R_2} is rotated $90°$ and interferes with anti-clockwise propagating beam E_{2R_1} at the output port of the loop mirror. Passing through the 50/50 fused coupler, one of the beam that travels across the waveguide in the coupler may experience phase lag of $\frac{\pi}{2}$. Thus, the overlap spectral at the output is expressed as

$$
\begin{aligned}
E_{\mathrm{OUT}} = & \; E_x e^{j(\phi_{1x}+\phi_{2x})}\cos\theta + E_y e^{j(\phi_{1y}+\phi_{2x})}\sin\theta \\
& + j\left(-E_x e^{j(\phi_{1x}+\phi_{2y})}\sin\theta + E_y e^{j(\phi_{1y}+\phi_{2y})}\cos\theta \right)
\end{aligned} \qquad (10)
$$

The detected output spectral power can be expressed as

$$P_{\mathrm{OUT}} = E_{\mathrm{OUT}} E_{\mathrm{OUT}}^* \qquad (11)$$

where $*$ denotes the complex conjugation. The final normalized spectral function of the loop mirror is obtained as;

$$
\begin{aligned}
P_{\mathrm{OUT}}(\lambda,\theta) = & \; \frac{1}{2}\left(\cos^2\theta \sin\left[\frac{2\pi\Delta n(L_1+L_2)}{\lambda}\right] \right. \\
& \left. + \sin^2\theta \sin\left[\frac{2\pi\Delta n(L_1-L_2)}{\lambda}\right] + 1 \right)
\end{aligned} \qquad (12)
$$

where $\Delta n = n_x - n_y$ denotes the difference between the fast-axes and slow-axes refractive index, $P_{\text{OUT}}(\lambda, \theta) \in [0, 1]$ and $\theta \in [0°, 90°]$.

Consider a scenario when there is no rotation of the birefringence axes $\theta = 0°$, the second term of the Eq. (12) is nulled. A comb-like transmission spectrum is acquired and the wavelength spacing of the spectrum is given by

$$\Delta\lambda_{0°} = \frac{\lambda^2}{\Delta n(L_1 + L_2)} \tag{13}$$

On the other hand when $\theta = 90°$, the first term of the function is suppressed and the wavelength spacing is given by

$$\Delta\lambda_{90°} = \frac{\lambda^2}{\Delta n \, |L_1 - L_2|} \tag{14}$$

From the analysis above, the transmission spectrum is a combination of the two comb-like spectrums which are governed by the functions $\sin^2 \theta$ and $\cos^2 \theta$. The total Hi-Bi fiber $L_1 + L_2$ is always larger than $|L_1 - L_2|$ which induces that $\Delta\lambda_{0°} < \Delta\lambda_{90°}$. As the angle of rotation becomes larger, transmission spectrum is transforming from small wavelength spacing $\Delta\lambda_{0°}$ into a larger wavelength spacing $\Delta\lambda_{90°}$ transmission spectrum.

3. RESULT AND DISCUSSION

The transmission spectrum of the FLM is simulated using the theory described at the previous section, which the results are compared with the experimental results. In the experiment, the transmission spectrum of the loop mirror is determined by injecting an amplified spontaneous emission (ASE) (1480 nm–1580 nm) source generated by a semiconductor optical amplifier (SOA) into the FLM through the input port of the experimental setup as illustrated in Fig. 1. The transmission from the loop mirror is analyzed using an OSA. Figs. 2–4 show the comparison between the analytical results and experimental results for different combinations of Hi-Bi fiber lengths, L_1 and L_2. For simplicity of the comparison, the waveguide losses in the experimental setup are compensated and the analytical result is computed based on lossless condition. The effect of this compensation on the result is expected to be very small and ignorable. In both experiment and theoretical simulation, Δn is set at 4.1×10^{-4}, L_1 is varied from 1.1 to 1.6 m and L_2 is varied from 1.6 to 3.9 m. In each fiber length combination, the calculation and experimental measurement are carried out for five

consecutive angles of rotation with step size of 22.5° in relation with the birefringence axes.

From Figs. 2–4, we observed that the experimental spectra are in good agreement with the theoretical spectra, verifying our theoretical model. However, a small discrepancy between the experiment and theory is observed due to the imperfection of polarization adjustment
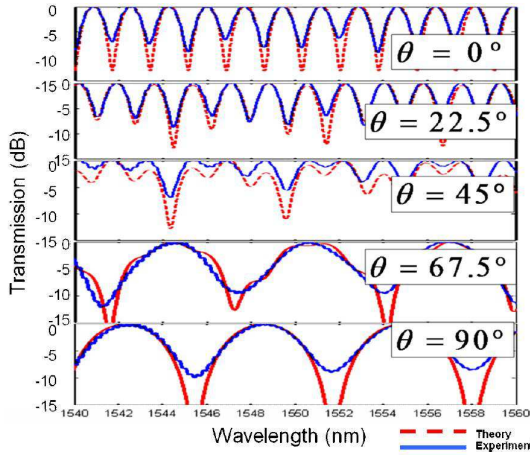
Figure 2. Transmission spectrum for various rotation angles when $L_1 = 1.2\,\text{m}$ and $L_2 = 2.1\,\text{m}$ ($\Delta n = 4.1 \times 10^{-4}$, $\Delta\lambda_{0°} = 1.71\,\text{nm}$, $\Delta\lambda_{90°} = 6.11\,\text{nm}$).
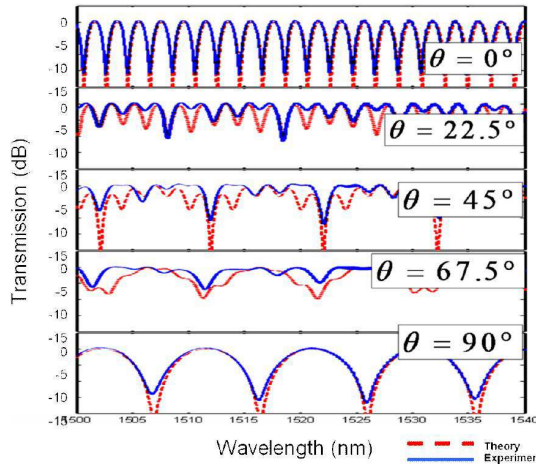
Figure 3. Transmission spectrum for various rotation angles when $L_1 = 1.1\,\text{m}$ and $L_2 = 1.6\,\text{m}$ ($\Delta n = 4.1 \times 10^{-4}$, $\Delta\lambda_{0°} = 2.05\,\text{nm}$, $\Delta\lambda_{90°} = 9.63\,\text{nm}$).
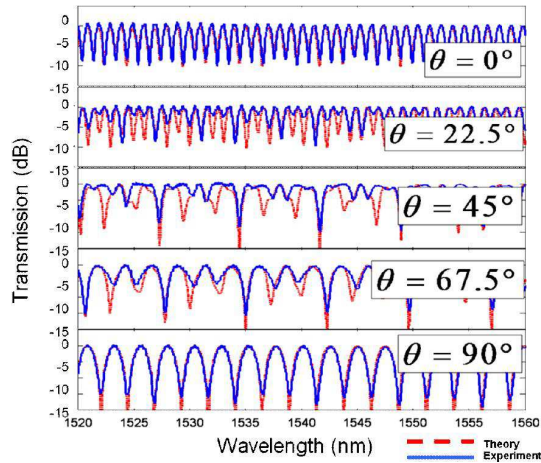
Figure 4. Transmission spectrum for various rotation angles when $L_1 = 1.6\,\text{m}$ and $L_2 = 3.9\,\text{m}$ ($\Delta n = 4.1 \times 10^{-4}$, $\Delta\lambda_{0°} = 1.01\,\text{nm}$, $\Delta\lambda_{90°} = 2.44\,\text{nm}$).

by PC2. In overall, Eq. (12) has exhibited as good function for the representation of the FLM transmission spectrum. At angles of $0°$ and $90°$, the FLM shows a uniform amplitude comb filter as shown in Figs. 2–4. The wavelength interval can be switched by changing the rotation angle from $0°$ to $90°$. For instance, the spacing can be changed from $1.71\,\text{nm}$ to $6.11\,\text{nm}$ when the lengths L_1 and L_2 of the FLM are set at $1.2\,\text{m}$ and $2.1\,\text{m}$ respectively. The results show that at different rotation angle of birefringence axes, interesting comb patterns can be obtained in the transmission spectrum due to different composition of two different comb-patterns as mentioned in the previous section. The variation of the output powers between the pass band and stop band is observed to be less than $10\,\text{dB}$ which is due to the unoptimised Hi-Bi fiber length.

4. CONCLUSION

The transmission function of the FLM with two-stage Hi-Bi fibers is theoretically and experimentally investigated in relation with the rotation angle of the fiber birefringence axes and fiber segments length. The theoretical transmission function of this FLM is calculated in detail by Jones Matrix. The experimental spectra are observed to be in good agreement with the theoretical spectra, verifying our theoretical model. The wavelength interval of the comb filter depends

on the Hi-Bi fiber lengths and rotation angles. By varying the rotation angle from 0° to 90°, a comb-like transmission spectrum with small wavelength spacing is evolving into an exotic but periodic transmission spectrum and eventually become a larger wavelength spacing transmission spectrum. This interesting property can be useful in optical signal processing, switches, power equalization and management for WDM network.

REFERENCES

1. Wu, J.-W., X.-D. Tian, and H.-B. Bao, "A designed model about amplification and compression of picosecond pulse using cascaded soa and NOLM device," *Progress In Electromagnetics Research*, PIER 76, 127–139, 2007.

2. Drexler, P., P. Fiala, and R. Kadlec, "Utilization of faraday mirror in fiber optic current sensors and experiments," *PIERS Proceedings*, 137–141, Beijing, China, 2009.

3. Hu, S., L. Zhan, Y. J. Song, W. Li, S. Y. Luo, and Y. X. Xia, "Switchable multiwavelength erbium-doped fiber ring laser with a multisection high-birefringence fiber loop mirror," *IEEE Photon. Technol. Lett.*, Vol. 17, 1387–1389, 2005.

4. Jinno, M. and T. Matsumoto, "Nonlinear Sagnac interferometer switch and its applications," *IEEE J. Quantum Electron.*, Vol. 28, 875–882, 1992.

5. Mirza, M. A. and G. Stewart, "Theory and design of a simple tunable Sagnac loop filter for multiwavelength fiber lasers," *Appl. Opt.*, Vol. 47, 5242–5252, 2008.

6. Dong, X. P., S. Li, K. S. Chiang, M. N. Ng, and B. C. B. Chu, "Multiwavelength erbium-doped fibre laser based on a high-birefringence fibre loop mirror," *Electron. Lett.*, Vol. 36, 1609–1610, 2000.

7. Liu, Y., B. Liu, X. Feng, W. Zhang, G. Zhou, S. Yuan, G. Kai, and X. Dong, "High-birefringence fiber loop mirrors and their applications as sensors," *Appl. Opt.*, Vol. 44, No. 12, 2382–2390, 2005.

8. Sun, G., D. S. Moon, and Y. Chung, "Simultaneous temperature and strain measurement using two types of high-birefringence fibers in Sagnac loop mirror," *IEEE Photon. Technol. Lett.*, Vol. 19, No. 24, 2027–2029, 2007.

9. Sun, G. and Y. Chung, "Simultaneous measurement for temperature and strain by use of Sagnac interferometer with controlled sensitivity," *Proc. SPIE*, Vol. 7004, 70041Y, 2008.